Online Control of Deposited Geometry of Multi-layer Multi-bead Structure for Wire and Arc Additive Manufacturing

Qinglin Han, Yongzhe Li, and Guangjun Zhang(✉)

Harbin Institute of Technology, West Da-Zhi Street 92,
Harbin 150001, People's Republic of China
zhanggj@hit.edu.cn

Abstract. A robotic wire and arc additive manufacturing (WAAM) system with active vision sensing capability was implemented to improve the geometry accuracy of multi-layer multi-bead structures. Width and height of the deposited bead were online detected and the accuracies of the designed sensing approaches are 0.25 mm and 0.1 mm, respectively. A double-input-double-output controller with two subsystems was designed to ensure the uniformity of bead width and bead height. The bead width was adjusted by a single neuron self-learning PI controller, while the bead height was controlled based on a rule-based engine. The experimental results indicated that (i) accuracy of the deposited bead width is controlled in 0.5 mm, (ii) accumulation effect of the bead height deviations has disappeared when multiple layers are overlapped, and (iii) the surface finish of each layer was controlled to be flat as well.

Keywords: Wire and arc additive manufacturing · Multi-layer multi-bead structure · Active vision sensing · Bead geometry control

1 Introduction

Additive manufacturing (AM) is a technology to fabricate parts by depositing material on a layer-by-layer basis. AM is capable to realize complex structure design and fabrication, and reduces material and energy at the same time [1, 2]. Wire and arc additive manufacturing (WAAM) is an alternative AM approach for metallic part deposition. The heat source of WAAM is welding arc, while the fed material is wire. It has been proved that WAAM requires lower cost on implementations and fabricates parts with higher efficiency in comparison with other metallic AM technics [3]. The research activities of WAAM regarding advanced material shaping, microstructure and mechanical performance analysis of the deposited part, and path optimization techniques have been reported in the literature succession [4–6].

In general, WAAM contains a planning phase and a deposition phase. In the planning phase, a 3D model of the target part is sliced into multiple layers. For each layer, the deposition path is designed based on the contour of the layer. In addition, manufacturing parameters are deduced according to the planned bead geometries of the layers.

S. Chen et al. (eds.), *Transactions on Intelligent Welding Manufacturing*,
Transactions on Intelligent Welding Manufacturing, DOI 10.1007/978-981-10-5355-9_7

However, geometries of the deposited bead are susceptible to be influenced by the diverse heat sinking conditions and thermo-mechanical coupling effects, which might cause deviations on the bead geometries to the planned values [7, 8]. When the deviations accumulate, the subsequent deposition process cannot advance strictly as planned. Therefore, the WAAM process has the fatal shortcomings of poor continuity and low accuracy.

Improving the accuracy of bead geometry is one of the research challenges in WAAM. To this end, online sensing and control is an efficient way to adjust the bead geometries according to the planned values. The research focusing on process control of WAAM is relative few. Most of the research reported in the literature focused on multi-layer single-bead structures [9, 10]. The work related to multi-layer multi-bead structures is a new research challenge.

This paper aims at improving the geometry accuracy of multi-layer multi-bead structures fabricated by WAAM. A line-structured light vision sensor was employed to measure the bead geometries online. A hybrid controller was designed and implemented to control the bead width and height. The proposed approach was validated by an experiment: fabrication of a multi-layer two-bead structure.

2 System Overview

A WAAM system based on GMAW was designed as shown in Fig. 1. It contains a Motoman HP20D robot, a Panasonic YD500FR welding machine, a GMAW torch, a META SLS-050 line-structured laser sensor, a computer, and some modules for signal transmission. The computer is the core of the system to ensure the coordination of the system components. It receives the stripes aggregated from the sensor, while sending control commands to adjust the manufacturing parameters in the deposition phase. The experimental materials and range of deposition parameters used in this paper are shown in Tables 1 and 2, respectively.

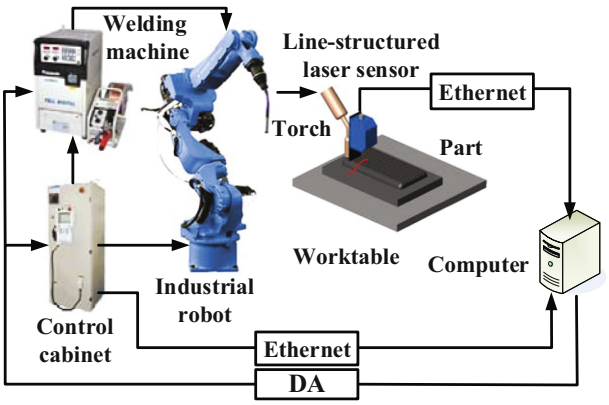

Fig. 1. Schematic diagram of the WAAM system

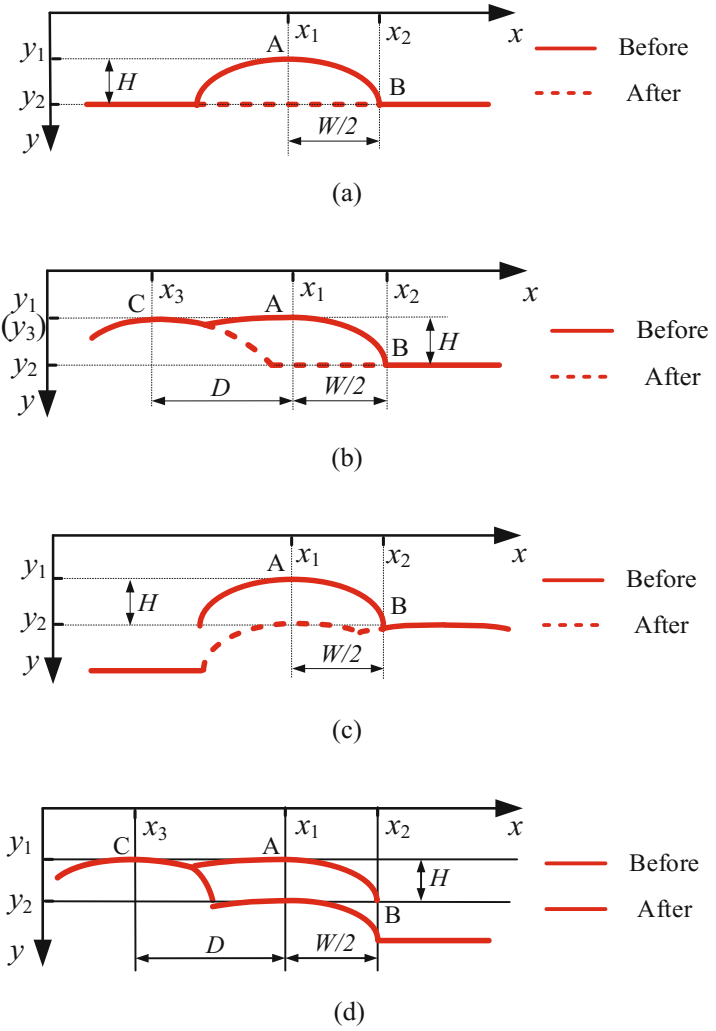

Fig. 2. Typical features of the light stripe of the deposited bead: (a) single bead; (b) overlapped bead; (c) first bead of a lapped layer; (d) last bead of a lapped layer

Table 1. Experimental materials

Substrate		Wire		Shielding gas	
Component	Thickness *t*/mm	Component	Diameter *d*/mm	Component	Flow *f*/(L/min)
Q235 steel	10	H08Mn2Si steel	1.2	95%Ar 5%CO_2	18

Table 2. Range of deposition parameters

Deposition current *I*/A	Deposition voltage *U*/V	Deposition speed *v*/(mm/s)
120–180	20–24	4–8

The reported data of the sensor indicates the cross-sectional profile of the surface of the deposited part. Based on the reported data, an image processing algorithm was designed to acquire the deposited bead geometries. The algorithm includes multiple steps regarding data preprocessing, pattern recognition and feature points extraction (vertex and toe of bead). Based on the designed algorithm the bead geometries are calculated, including bead height (H) and bead width (W). The extracted features of deposited beads are shown in Fig. 2. The detection error of H is ±0.1 mm, while the detection error of W is ±0.25 mm.

3 Controller Design

The objective of the controller is to keep H and W of any deposited bead to the planned values: H_{set} and W_{set}. However, H and W are strongly coupled, which implies that the adjustment of any manufacturing parameter, e.g. deposition voltage (U), deposition current (I) and deposition speed (v), changes both H and W at the same time. To solve this problem, it is necessary to separate the control of the width and height into two sub-controllers. A hybrid controller was developed and is shown in Fig. 3, which controls the W as the main goal and controls the H as the second goal.

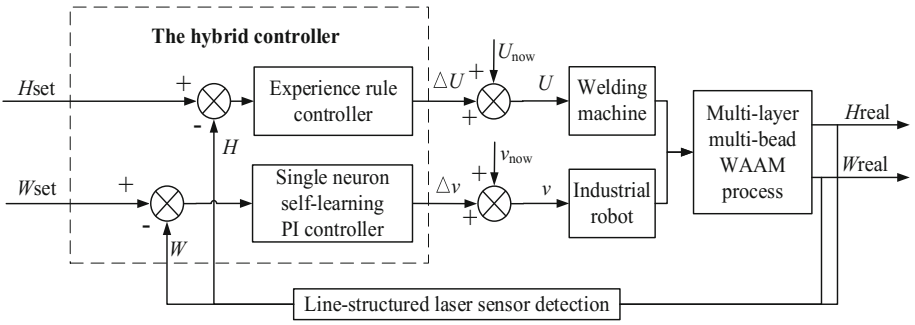

Fig. 3. Schematic diagram of the developed hybrid controller

In this controller, two sub-controllers are combined and work cooperatively. The first sub-controller is used to control W by adjusting v with a single neuron self-learning PI controller, since W is sensitive to the change of velocity. The pure delay of the sensing system was taken into consideration. That is the reason why the differential term of the PID controller is forbidden to avoid oscillation of W. In addition, the single neuron with learning capability was employed to self-tune the PI parameters during the control process based on the learnt experience. The learning capability enables the PI controller

adaptive to the complex WAAM deposition process with high robustness. Furthermore, the objective of the second sub-controller is to prevent the accumulation of H deviations. It works by trimming U with the following experience rules in a low adjusting frequency:

$$\mathrm{R1}: \mathrm{IF} H_{set} - H > 0.2 \ \ \mathrm{THEN} \ \ U_{n+1} = U_n - 0.5 \tag{1}$$

$$\mathrm{R2}: \mathrm{IF} H_{\mathrm{set}} - H < -0.2 \ \mathrm{THEN} \ \ U_{n+1} = U_n + 0.5 \tag{2}$$

$$\mathrm{R3}: \mathrm{IF} -0.2 \leq H_{\mathrm{set}} - H \leq 0.2 \ \ \mathrm{THEN} \ \ U_{n+1} = U_n \tag{3}$$

4 Experimental Results and Discussion

An open-loop experiment and a closed-loop experiment to fabricate a multi-layer multi-bead structure were planned as comparative experiments to validate the developed controller. The target structure was a cuboid component with the cross-sectional size of 13 mm (component width) × 12.6 mm (component height). The component was designed with 6 layers and 2 overlapped beads in each layer. The planned bead geometries are shown in Table 3. The initial deposition parameters were set as following: the deposition current was 150A, the deposition voltage was 22 V, and the deposition speed was 5 mm/s.

Table 3. The planned bead geometries

Layer	Bead height/mm	Bead width/mm	Center distance/mm	Layer width/mm
1	2.6	7.5	5.5	13
2–6	2.0	7.5	5.5	13

In the open-loop deposition process, the deposition parameters of all beads were kept as the initial values. The detected H and W of several beads are shown in Fig. 4. For simplicity, W_{ij} and H_{ij} are referred to as W and H of the jth bead of the ith layer. It can be seen from Fig. 4 that W_{ij} gets larger while the number of layer increases. In addition, H_{i2} in each layer is higher than H_{i1} when $i > 2$. The heat sinking conditions of the beads in a layer ($i > 2$) is worse than those of the layers below, which results in a lower cooling rate and a longer duration at high temperature of each bead in the layer. That is the reason why bead width increases when the number of layer increases. As a consequence, the center distance between the deposited beads in the second and above layers mismatches to the geometries of the beads, which causes deviation of H.

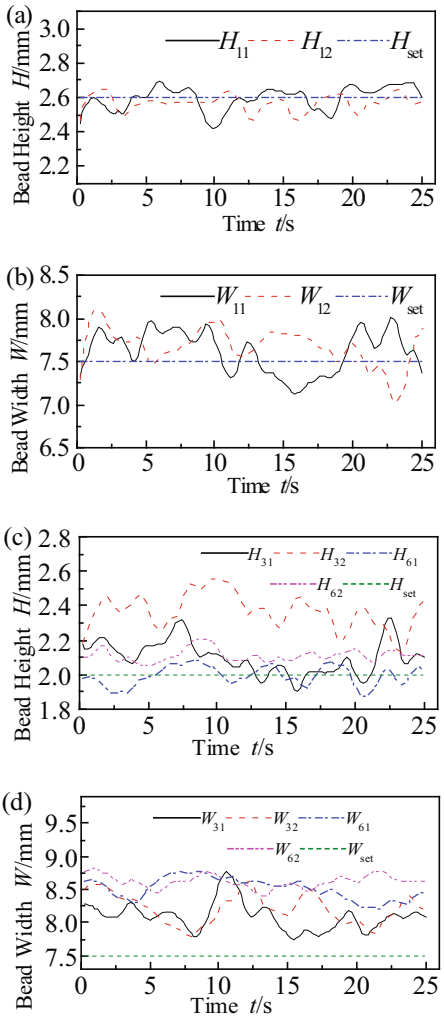

Fig. 4. Detected values in the open-loop deposition experiment: (a) H_{1j}; (b) W_{1j}; (c) H_{3j} and H_{6j}; (d) H_{3j} and H_{6j}, $j = 1, 2$

In the closed-loop deposition experiment, the developed controller was used. The control commands were developed for keeping the bead geometries as planned. The control cycle of W is 2 s, and that of H is 5 s. The detected values of the manufacturing parameters and bead geometries are shown in Fig. 5. With the proposed controller, W was kept to be stable around the planned value, while H deviation is smaller than that in the open-loop experiment. The accuracy of W in the controlled section was better than 0.5 mm.

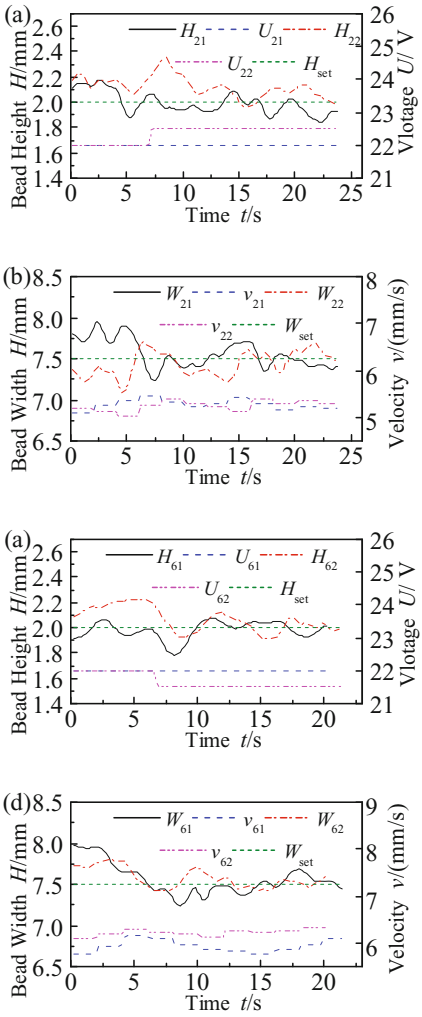

Fig. 5. Detection curve of closed-loop deposited bead sizes: (a) W of the 2nd layer 1st bead; (b) H of the 2nd layer 2nd bead; (c) W of the 6th layer 1st bead; (d) H of the 6th layer 2nd bead

The cross-sectional profiles of the deposited parts in the experiments are shown in Fig. 6. The width deviation of the deposited part in the open-loop experiment is up to 1.24 mm (9.5% of the layer width), while that in the closed-loop experiment was 0.52 mm (4% of the layer width). Furthermore, the top surface of the structure fabricated in the closed-loop experiment is smoother as well. The results indicated that the controller designed in this paper is suitable to improve the geometry accuracy of multi-layer multi-bead structures fabricated by WAAM.

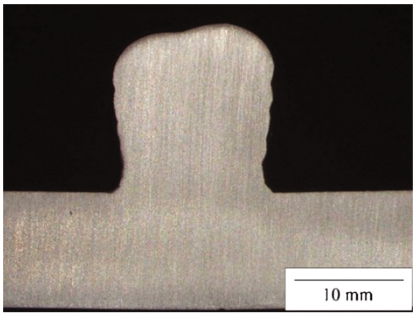

(a)

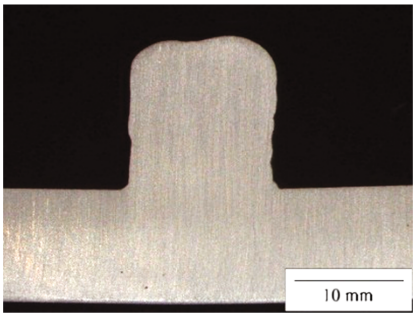

(b)

Fig. 6. Section of the formed structures: (a) open-loop experiment; (b) closed-loop experiment

5 Conclusions

A robotic WAAM system with an active vision sensor and a hybrid controller has been built for fabrication of multi-layer multi-bead structures. The conclusions are:

- The active vision sensor is able to detect the cross-sectional profile of a deposited bead in a multi-layer multi-bead structure. Based on the proposed image processing algorithm for extracting feature points of light stripes, the W and H of a deposited bead are known. The detection error of H is less than 0.1 mm, while that of W is less than 0.25 mm.
- The designed controller is suitable to keep the bead geometries as planned. The error on W is controlled within 0.5 mm. The controller also prevents accumulation of H deviations, which results in a flat surface of the fabricated structure.

Acknowledgement. The authors would like to thank Prof. Hongming GAO for his support on the implementation of the robotic WAAM system and Mr. Dongqing YANG for his technical assistant. This work was supported by National Natural Science Foundation of China, No. 51575133.

References

1. Pinto J, Arrieta C, Andia M et al (2015) Sensitivity analysis of geometric errors in additive manufacturing medical models. Med Eng Phys 37(3):328–334
2. Zhong X, Teoh J, Liu Y et al (2015) 3D printing of smart materials: a review on recent progresses in 4D printing. Virtual Phys Prototyping 10(3):103–122
3. Xiong J, Zhang G, Zhang W (2015) Forming appearance analysis in multi-layer single-pass GMAW-based additive manufacturing. Int J Adv Manufact Technol 80(9):1767–1776
4. Almeida P, Williams S (2010) Innovative process model of Ti–6Al–4 V additive layer manufacturing using cold metal transfer (CMT). In: Proceedings of 21st Annual International Solid Freeform Fabrication Symposium, University of Texas at Austin, Austin, TX, USA, pp 25–36
5. Kazanas P, Deherkar P, Almeida P et al (2012) Fabrication of geometrical features using wire and arc additive manufacture. Proc Inst Mech Eng Part B J Eng Manufact 226(6):1042–1105
6. Ding D, Pan Z, Cuiuri D et al (2016) Adaptive path planning for wire-feed additive manufacturing using medial axis transformation. J Clean Prod 133:942–952
7. Zhao H, Zhang G, Yin Z et al (2012) Three-dimensional finite element analysis of thermal stress in single-pass multi-layer weld-based rapid prototyping. J Mater Process Technol 212(1):276–285
8. Ding D, Shen C, Pan Z et al (2016) Towards an automated robotic arc-welding-based additive manufacturing system from CAD to finished part. Comput Aided Des 73:66–75
9. Doumanidis C, Kwak YM (2002) Multivariable adaptive control of the bead profile geometry in gas metal arc welding with thermal scanning. Int J Press Vessels Pip 79(4):251–262
10. Xiong J, Zhang G (2014) Adaptive control of deposited height in GMAW-based layer additive manufacturing. J Mater Process Technol 214(4):962–968